Chapter 5

RESULTS AND DISSCUSSION

5.1 Adsorbent Characteristics

Adsorbent characteristics were inspected visually with scanning electron microscope (SEM), and were also examined with x-ray diffraction (XRD) and with adsorption of gaseous nitrogen at its normal boiling point. In addition, chemical composition of each adsorbent was analysed. All results were discussed below.

5.1.1 Scanning Electron Microscope Results

External surface of unexpanded perlite was inspected visually with SEM, and was found that such perlite was nonporous, as illustrated in Figure 5.1. Whereas, the visual inspection of expanded perlite revealed a number of pores which were similar to exploded bubbles, as shown in Figure 5.2and Figure 5.3.

The pore size varied with the particle size of unexpanded perlite, i.e. the pore size decreased with decreasing particle size. Furthermore, on sufficiently small particle size, the shape of pore was not similar to bubble shape, as shown in Figure 5.4. These results suggested that a large particle might contain greater

Figure 5.1: Scanning Electron Microscope of Perlite before expansion

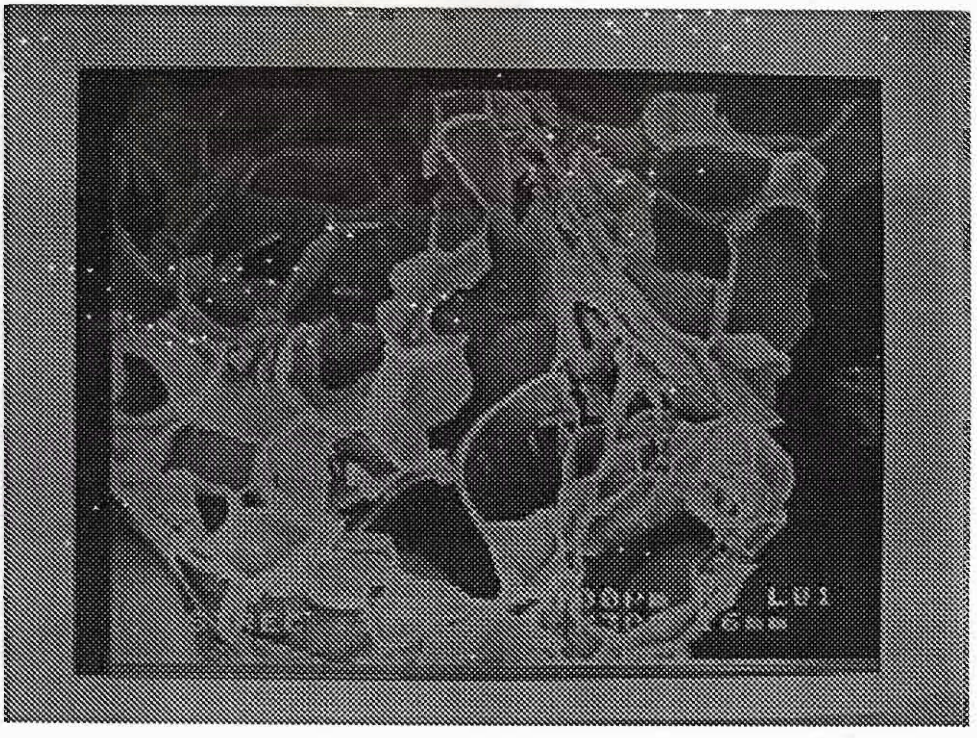

Figure 5.2: Scanning Electron Microscope of Expanded Perlite 40-60 mesh

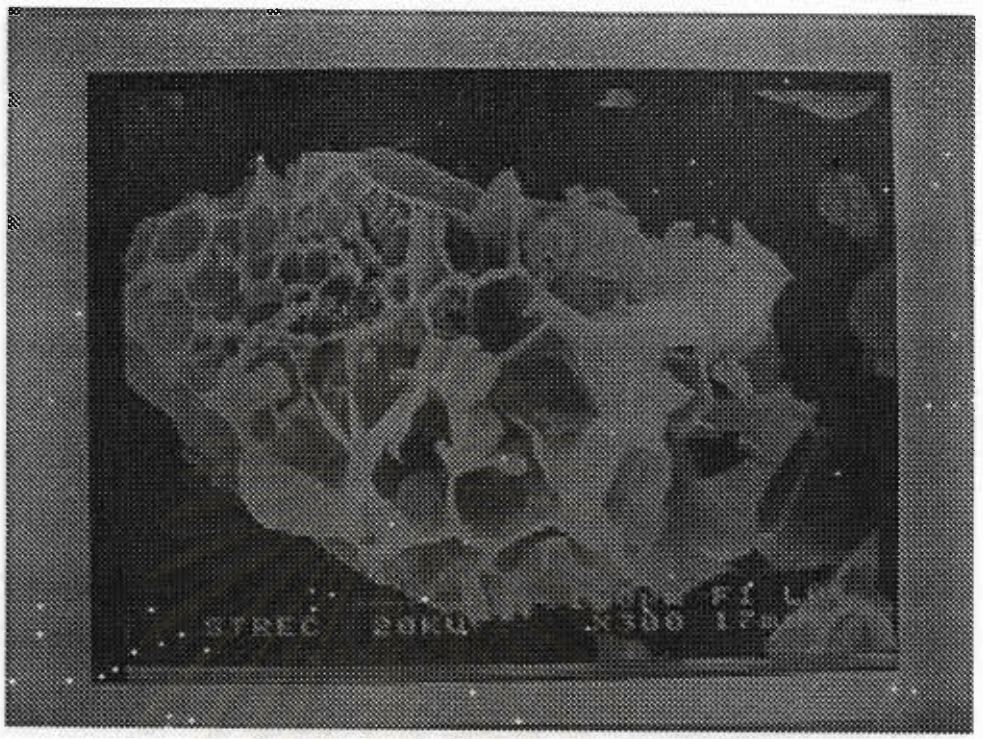

Figure 5.3: Scanning Electron Microscope of Expanded Perlite 60-80 mesh

portion of expandable compounds, such as water, than a small one. With sudden heating within extremely short period, e.g. a few ten seconds, such great portion of expandable compounds was able to produce larger bubble or pore size than the small one. While a sufficiently small portion of such compounds was not able to produce bubble-shape pore size. Furthermore, perlite might not be broken during the expansion process.

Figure 5.4: Scanning Electron Microscope of Expanded Perlite 80-100 mesh

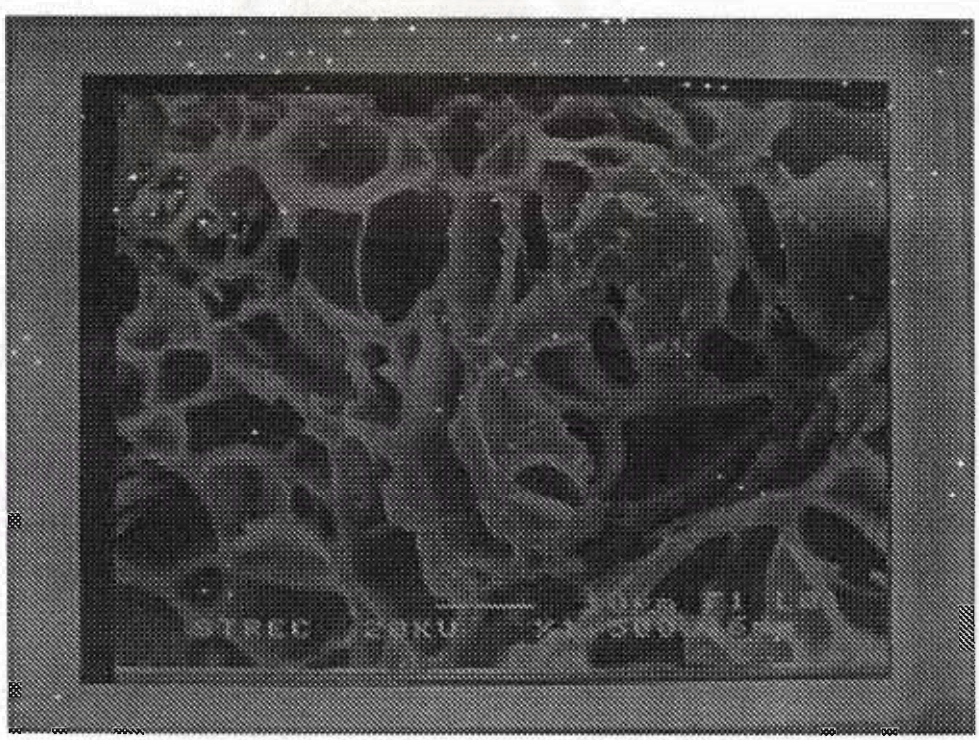

Figure 5.5: Scanning Electron Microscope of Expanded Perlite 80-100 mesh with higher magnification

Figure 5.6: Scanning Electron Microscope of Pumice 40-60 mesh

For pumice, a certain number of pores were found on each particle. Each pore was similar in shape and size, as shown in Figure 5.6, Figure 5.7, and Figure 5.8. In addition, the pores tended to extend longitudinally. Furthermore, the pore size was independence of particle sizes. In other words, the pores in a large particle were the same size as that in a small one.

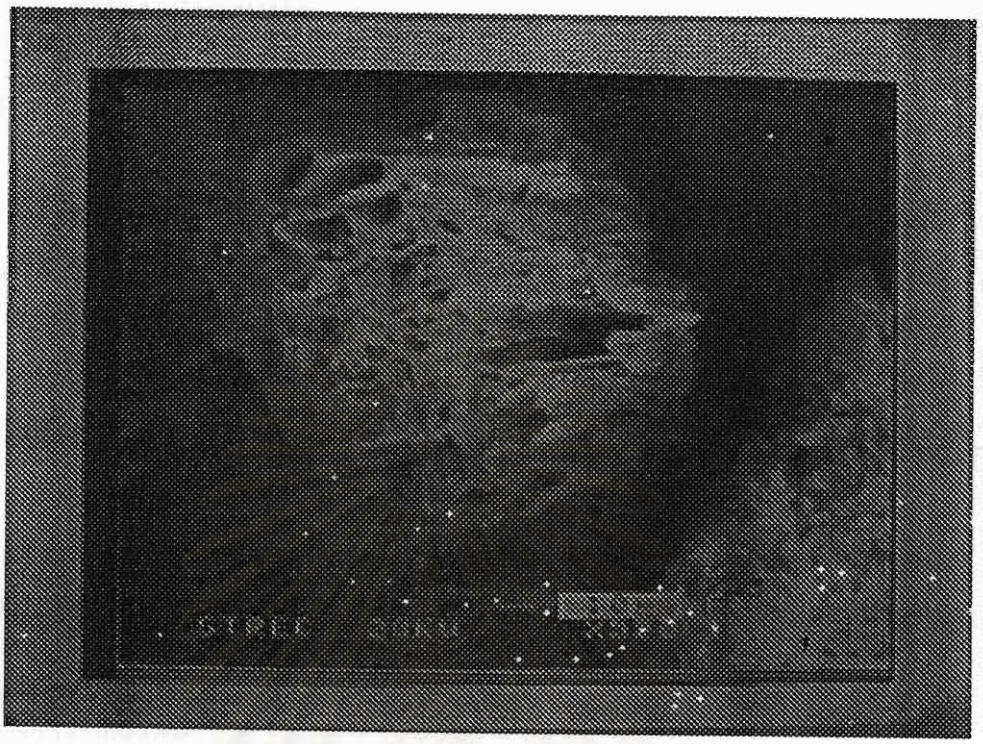

Figure 5.7: Scanning Electron Microscope of Pumice 60-80 mesh

Figure 5.8: Scanning Electron Microscope of Pumice 80-100 mesh

5.1.2 BET Results

Based on nitrogen adsorption of 77K, pumices provide higher specific surface area than perlites with the same mesh sizes, as summarized in Table 5.1. The surface areas of both pumices and perlites increase with an increase in the mesh size. In other words, small volcanic rocks provide high specific surface area. From the results of specific surface area of these natural adsorbents are lower values than synthetic adsorbents such as zeolites of which the surface area varies with types.

Table 5.1: The BET results of all sizes of Pumices and Perlites compared with commercial zeolite

Adsorbents	mesh size	BET surface area (m^2/g)	Pore size(Å)
Pumice	40-60 mesh	7.35	85.72
Pumice	60-80 mesh	12.82	82.22
Pumice	80-100 mesh	13.07	75.07
Perlite	40-60 mesh	1.54	106.21
Perlite	60-80 mesh	4.88	59.18
Perlite	80-100 mesh	9.80	43.82
Zeolite A	60-80 mesh	25.29	140.21
Zeolite X	60-80 mesh	481.13	19.10
Zeolite Y	60-80 mesh	721.33	15.21

In spite of the difference in specific surface areas, all pumices provide similar average pore size of 80Å, suggesting uniform formation of pumice. While the average pore size of expanded perlite increases as an increase in the size of particles. It might be the results of sudden expansion of volatile substances in raw perlites.

Table 5.2: Wet Chemical Analysis Result

Component (%)	Perlite before expanded	Perlite after expanded	Pumice
SiO_2	71.80	72.63	66.86
Al_2O_3	13.53	14.73	15.23
Fe_2O_3	1.26	1.31	1.37
TiO_2	0.04	0.05	0.17
CaO	0.95	1.58	1.17
MgO	0.14	0.27	0.91
Na_2O	2.13	2.04	1.09
K_2O	5.36	5.15	4.47
H_2O	0.31	0.49	1.97
LOI	4.53	1.80	6.32

5.1.3 Wet Chemical Analysis Results

From the wet chemical analysis results provided all of known components in these adsorbents. In case of perlite before and after expansion, composition of perlite was not altered, except the loss of ignition, as summarized in Table 5.2. The results suggested that both physical and chemical properties of perlite, except density, might not be altered by the thermal expansion within a very short period. In comparison with pumice, both volcanic rocks were composed of similar chemical composition which corresponded to the formation of the rocks after volcano eruption.

5.1.4 X-ray Diffraction Results

Although the chemical composition of pumice was similar to that of perlite, the forms of those composition in both rocks were different. A certain fraction of the metal oxides in pumice formed montmorillonite, according to the XRD results,

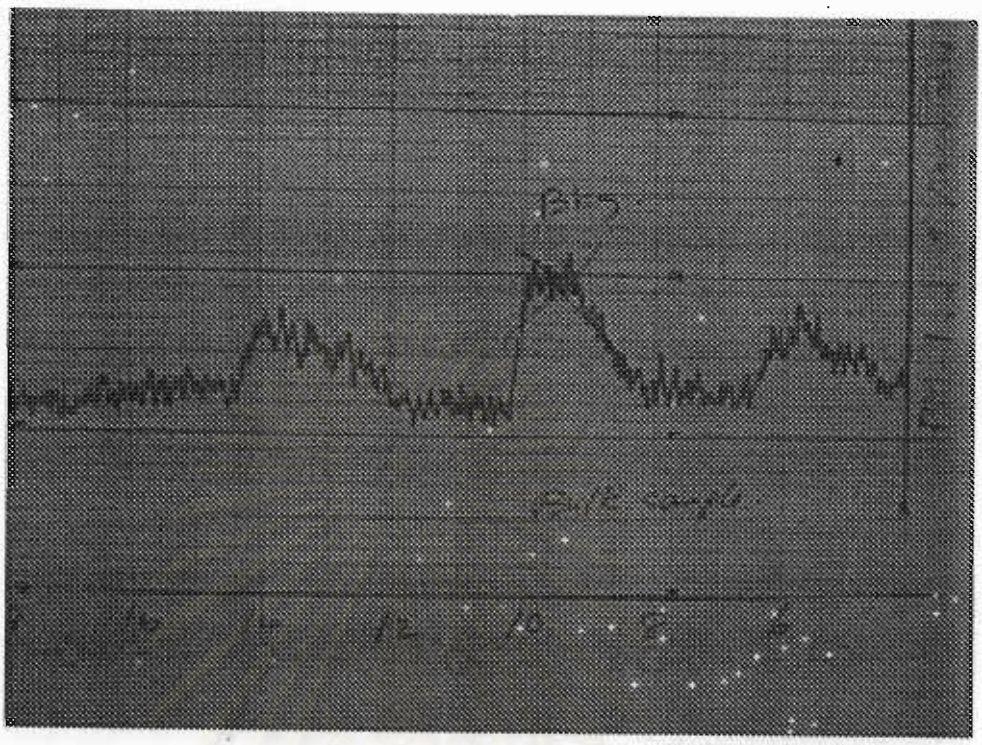

Figure 5.9: x-ray diffraction of pumice

as shown in Figure 5.9.

While none of the metal oxides formed known crystalline structure in Figure 5.10.

5.2 Column Characterization

Each column, packed with a selected volcanic rock for adsorption experiments was verified by the variation of pressure drop across the packed bed with the flow rate. Since the carrier gas was not adsorbed, the relationship of the pressure drop to the flow rate corresponded to Blake-Kozeny equation 4.2. as shown in Figure 5.11. The slope of each linear plot was close to -1. The intercept of the plot provided the information of bed porosity. The bed porosity was one of three

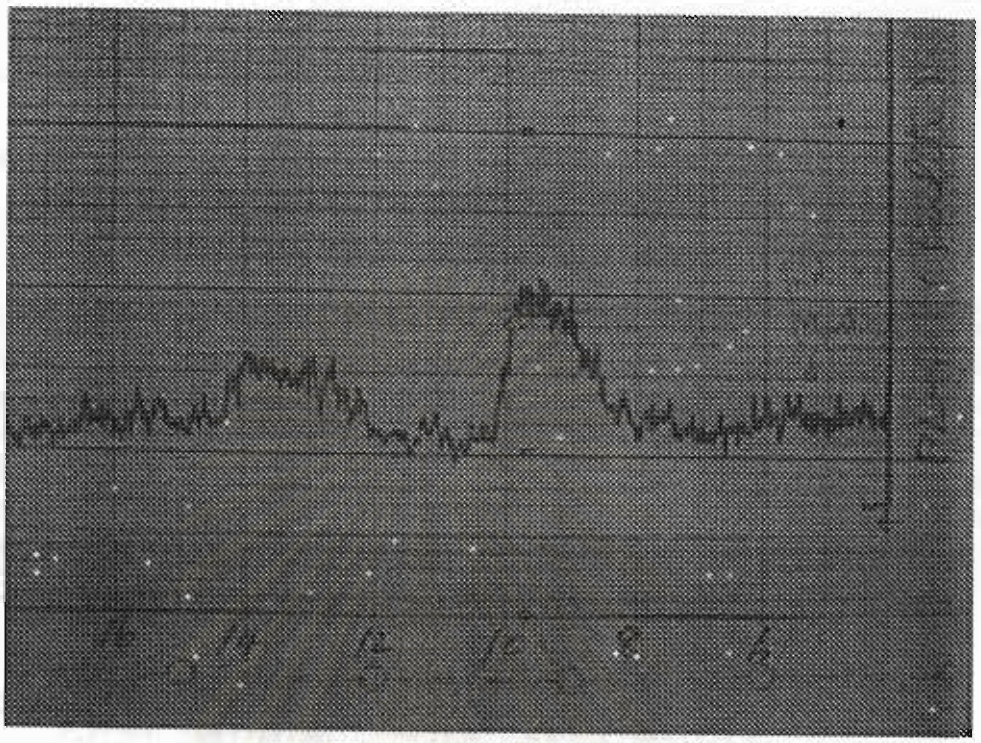

Figure 5.10: x-ray diffraction of perlite

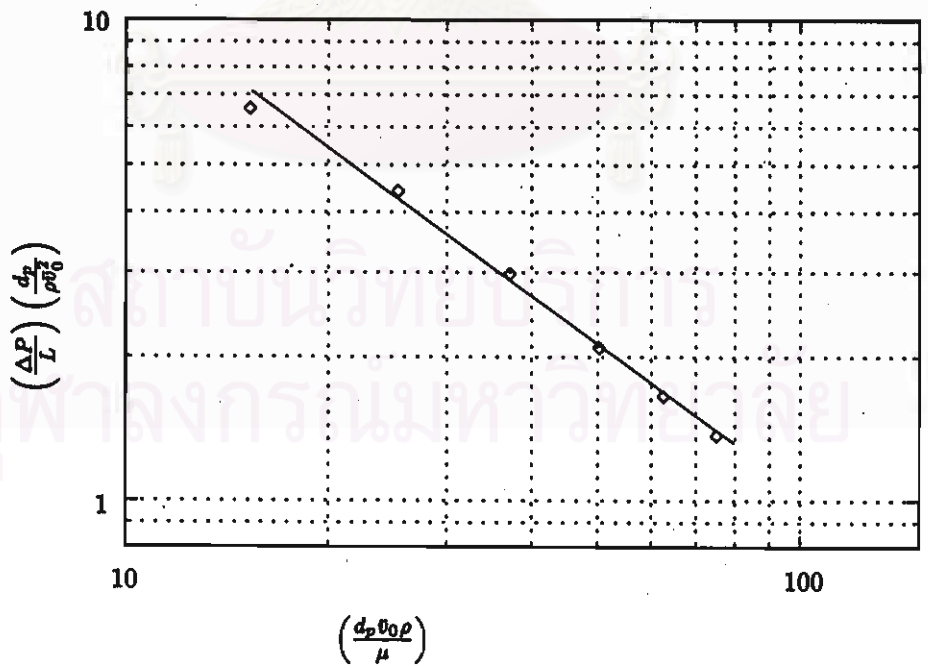

Figure 5.11: The sample of the plot of pressure and flowrate of pumice 40-60 mesh of 0.3 cm column length determine the bed porosity

available solutions obtained from the third degree polynomial expression. The particle density was determined from equation 4.3. The bed porosity and particle density for all packed columns were summarized in Table 5.3

Table 5.3: Characterization of Packed Column

Adsorbents	mesh size	Amount(g)	Bed Length(cm)	Porosity	Density
Pumice	40-60 mesh	0.0062	0.30	0.3759	0.2015
Pumice	60-80 mesh	0.0031	0.30	0.5577	0.1422
Pumice	80-100 mesh	0.0029	0.30	0.5636	0.1342
Perlite	40-60 mesh	0.7424	12.50	0.6041	0.9136
Perlite	60-80 mesh	0.9330	12.50	0.5045	0.9174
Perlite	80-100 mesh	0.5960	12.50	0.5722	0.6788

5.3 First Moment Analysis Results

5.3.1 An Adsorption Equilibrium Constant

For a given temperature, the weighted mean residence time (t_R) was proportional to the ratio of the bed length (L) to the gas velocity (v), as shown in Figure 5.12. According to equation 3.7, the adsorption equilibrium constant for the dilute solution was determined from the slope of the corresponding plots. All equilibrium constants were summarized in Table 5.4.

Each pair of adsorbate and adsorbent, the equilibrium constants varied inversely with temperatures. The relationship of the equilibrium constant to temperature corresponded to van't Hoff equation as shown in Figure 5.13 and Figure 5.14.

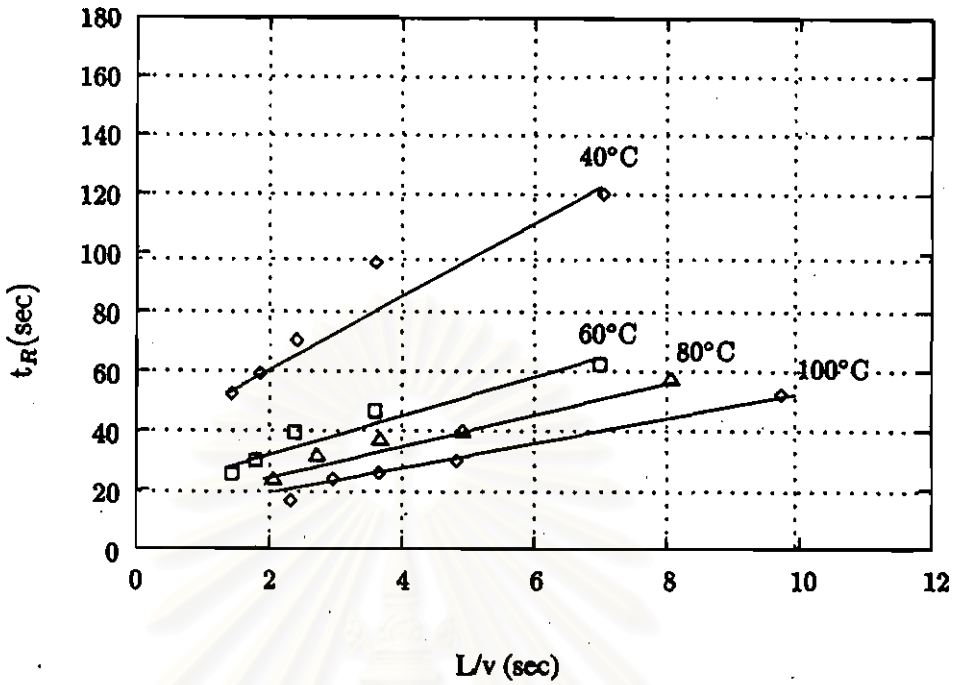

Figure 5.12: The first moment plot of adsorption of acetone on pumice 80-100 mesh at various temperature

Table 5.4: Adsorption equilibrium constants of toluene and acetone on both adsorbents at various temperature

Adsorbates	Temp	Pumice (mesh)			Perlite (mesh)		
	°C	40-60	60-80	80-100	40-60	60-80	80-100
Toluene	40	2189	1009	496	65.0	18.0	7.2
	50	1780	862	434	27.0	13.0	5.3
	60	965	690	380	17.0	6.8	4.3
	70	477	489	299	10.0	6.3	4.2
	80	446	383	257	8.0	5.1	4.0
	90	239	357	186	5.8	5.0	3.5
	100	229	227	139	5.0	3.0	3.0
	110	178	155	129	4.0	2.0	2.9
Acetone	40	2597	2300	963	41.0	25.0	15.0
	50	2121	1803	632	20.0	12.0	9.4
	60	1979	1773	565	19.0	10.4	7.1
	70	1096	1248	412	15.5	10.1	6.3
	80	1016	983	206	15.0	9.0	6.0
	90	760	768	184	14.0	7.4	5.3
	100	706	312	173	11.0	5.5	4.3
	110	267	285	165	6.4	5.4	4.0

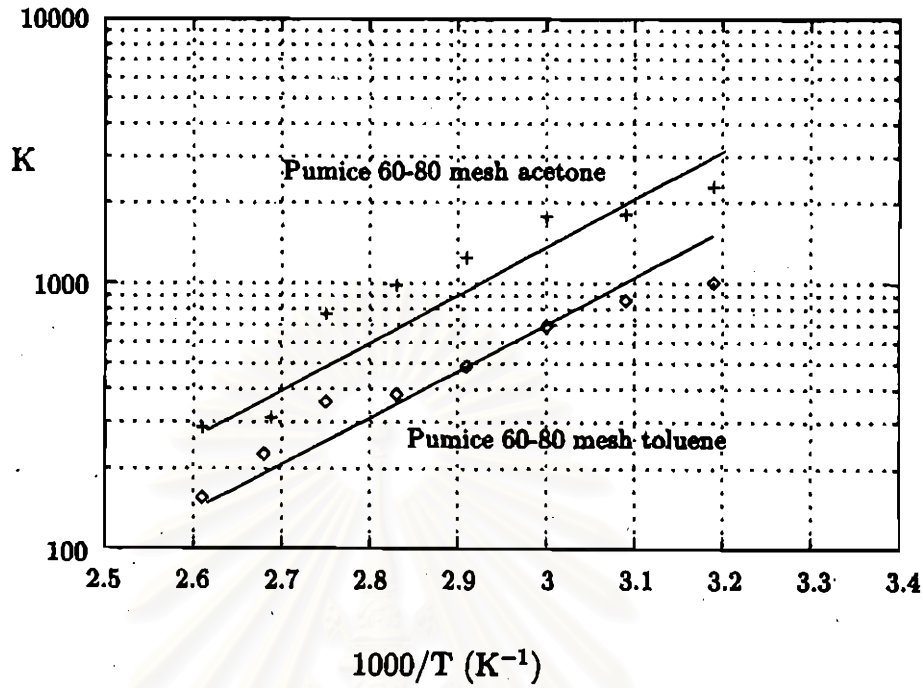

Figure 5.13: Adsorption equilibrium constants of acetone and toluene on pumice 60-80 mesh

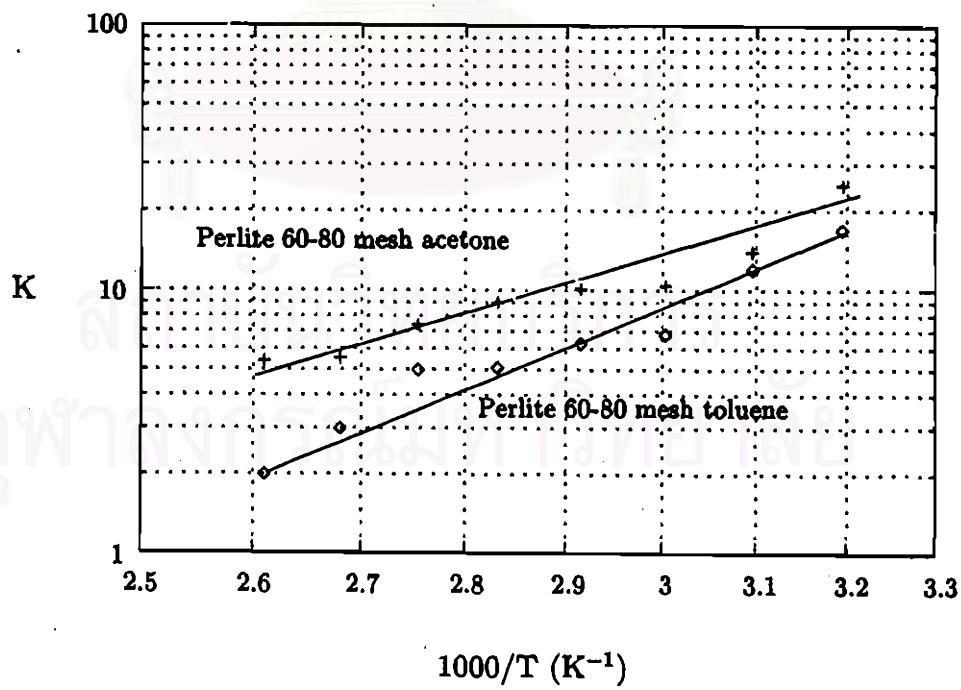

Figure 5.14: Adsorption equilibrium constants of acetone and toluene on perlite 60-80 mesh

Effects of Adsorbate Types

At a given temperature, the adsorption equilibrium constant of acetone on pumice was greater than that of toluene on the same adsorbent, as shown in Figure 5.13. On perlite, the equilibrium constant of acetone was also greater than that of toluene, as shown in Figure 5.14. The results suggested that both volcanic rocks, which were moderately hydrophilic [17], prefered adsorbing polar molecules, such as acetone, to adsorbing non-polar molecules, such as toluene.

Effects of Adsorbent Types

Although both volcanic rocks were composed of similar compounds of metal oxides, e.g. SiO_2, Al_2O_3 etc., as summarized in Table 5.2, such compounds were formed structural solid differently. Perlite was formed as conventional mixed solid of metal oxides, while pumice consisted of a certain fraction of crystalline solid, formed by such metal oxides, as explained previously. Consequently, the crystalline solid provided greater adsorption equilibrium constant than the non-crystalline one, especially for dilute solution of polar molecules such as acetone, as shown in Figure 5.15, in the same manner as the comparison of moisture adsorption on zeolite A with that on silica gel. In addition, since pumice was not expanded, adsorption occured mostly on the crystalline solid. For slightly polar molecules such as toluene, the crystalline solid in pumice still provided greater adsorption equilibrium constant than the non-crystalline one in perlite because of the available specific surface area, as shown in Figure 5.16.

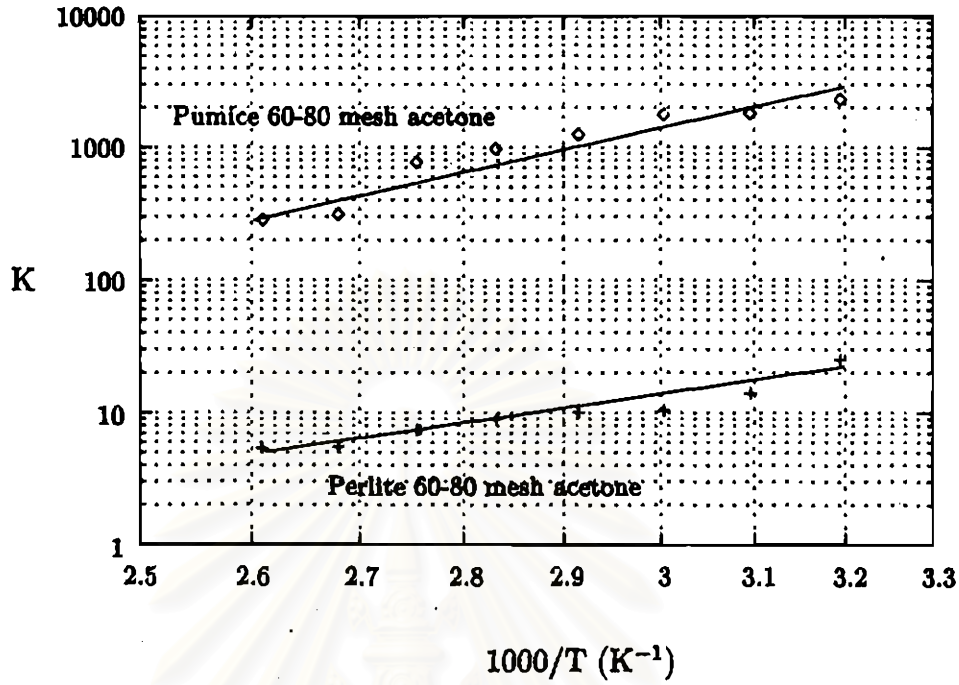

Figure 5.15: Adsorption equilibrium constants of acetone on perlite and pumice 60-80 mesh

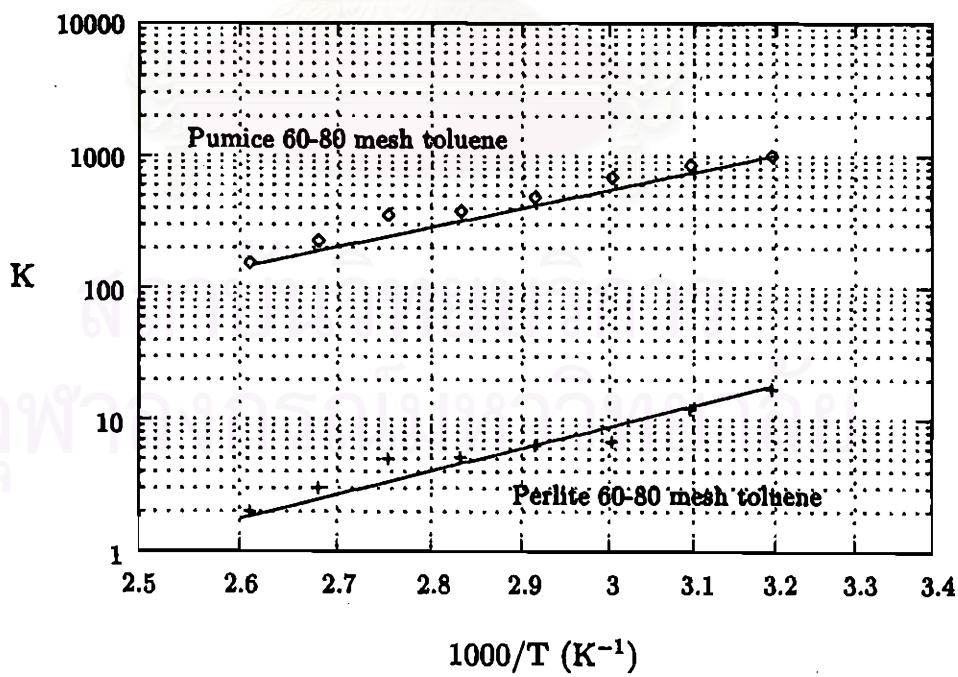

Figure 5.16: Adsorption equilibrium constants of toluene on perlite and pumice 60-80 mesh

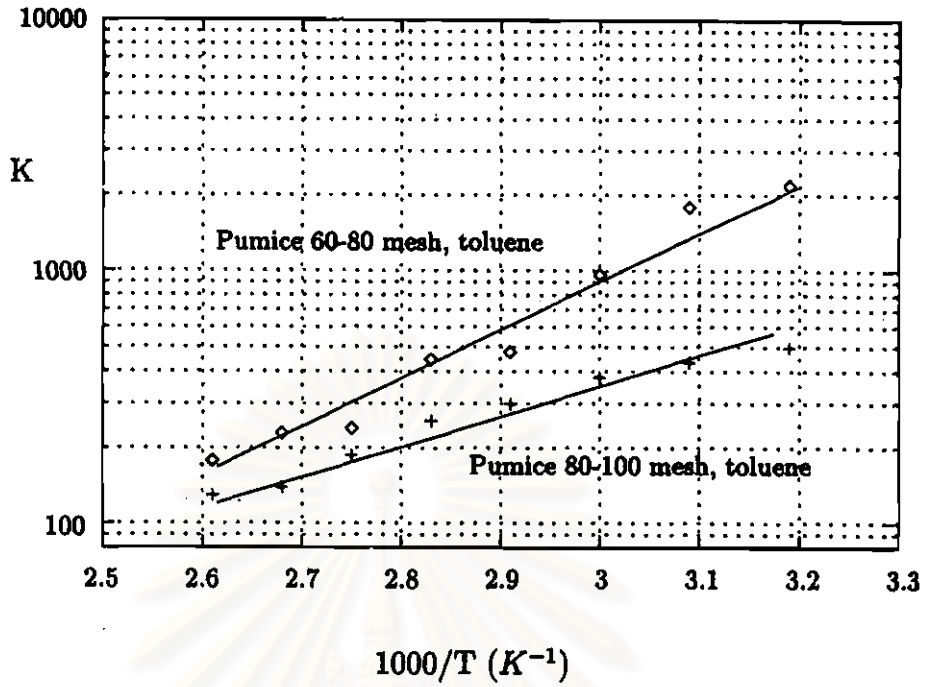

Figure 5.17: Adsorption equilibrium constant of toluene on pumices with different particle size

Effects of Sizes of Adsorbent

In spite of a relatively high specific surface area of small particles, based on adsorption of gaseous nitrogen, large particles provided greater equilibrium constant than small ones, as shown in Figure 5.17 and Figure 5.18.

Since the molecular sizes of both acetone and toluene were larger than that of nitrogen, the utilized pore volume or pore area had to related to the relative molecular size to the pore size. The results suggested that the large particles might provide more effective surface area of adsorption of acetone and toluene than the small particles.

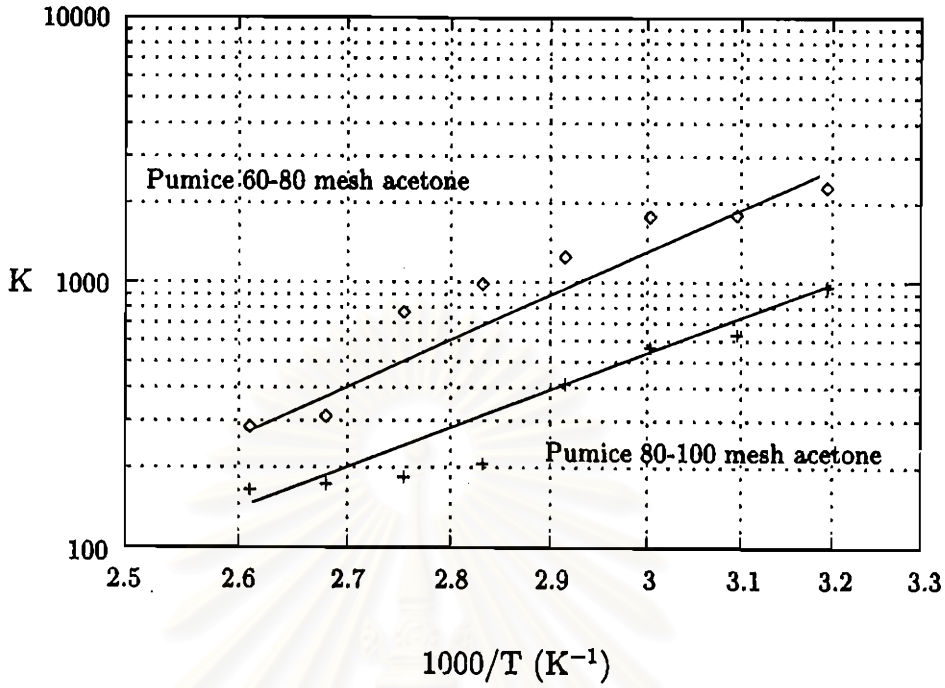

Figure 5.18: Adsorption equilibrium constant of acetone on pumice with different particle size

5.3.2 Heat of Adsorption

Since the variation of the adsorption equilibrium constant with temperature corresponded with the van't Hoff equation, the slope of the linear plot between the equilibrium constant and the reciprocal temperature in the semi-logarithmic scale provided the information of heat of adsorption. The results were summarized in Table 5.5

For adsorption of acetone, the heat of adsorption varied only with types of adsorbent. While the relatively high polarity on the surface of pumice, the heat of adsorption on pumice was higher than that on perlite.

However, it was found that the heat of adsorption of toluene varied with the sizes of adsorbents. Furthermore, adsorption on volcanic rocks did not relate

Table 5.5: Heat of adsorption of toluene and acetone vapors on perlite and pumice

Adsorbate	Adsorbents	Mesh size (mm)	-Δ H (kJ/mol)
Toluene	Pumice 40-60 mesh	0.32	20.57
	Pumice 60-80 mesh	0.21	25.96
	Pumice 80-100 mesh	0.16	38.37
	Perlite 40-60 mesh	0.32	12.21
	Perlite 60-80 mesh	0.21	27.10
	Perlite 80-100 mesh	0.16	38.01
Acetone	Pumice 40-60 mesh	0.32	27.42
	Pumice 60-80 mesh	0.21	29.44
	Pumice 80-100 mesh	0.16	30.18
	Perlite 40-60 mesh	0.32	17.15
	Perlite 60-80 mesh	0.21	18.70
	Perlite 80-100 mesh	0.16	20.11

to polarity of the surface.

5.4 Second Moment Results

5.4.1 Overall Mass Transfer Coefficients

According to equation 3.15, overall mass transfer coefficients for adsorption of acetone and toluene on both volcanic rocks were obtained from the intercept of the corresponding of the linear plot. The results were summarized in Table 5.6

On both selected volcanic rocks, the overall mass transfer coefficients for small particles were higher than the large ones, corresponding with the effects of particle sizes on the external film mass transfer coefficients.

In comparison between perlite and pumice, the mass transfer coefficients for

Table 5.6: Overall mass transfer coefficient of toluene and acetone on adsorbents at various temperature

Adsorbates	Temp	Pumice (mesh)			Perlite (mesh)		
	°C	40-60	60-80	80-100	40-60	60-80	80-100
Toluene	40	0.011	0.027	0.070	0.150	0.010	4.400
	50	0.015	0.035	0.073	0.340	0.290	5.700
	60	0.030	0.045	0.084	1.560	0.430	6.750
	70	0.053	0.050	0.110	1.840	0.960	7.530
	80	0.056	0.150	0.270	3.590	2.640	12.380
	90	0.084	0.167	0.320	6.054	2.710	16.200
	100	0.127	0.174	0.330	25.290	4.930	24.900
	110	0.124	0.190	0.350	37.240	5.030	37.790
Acetone	40	0.010	0.014	0.038	0.029	0.058	0.123
	50	0.012	0.015	0.058	0.047	0.068	0.174
	60	0.013	0.016	0.088	0.051	0.069	0.264
	70	0.020	0.022	0.126	0.075	0.070	0.500
	80	0.020	0.030	0.138	0.078	0.100	0.930
	90	0.024	0.034	0.192	0.086	0.111	1.280
	100	0.040	0.104	0.241	0.139	0.175	1.520
	110	0.071	0.106	0.297	0.157	0.230	3.280

perlite were higher than that pumice because of the shape and sizes of pores, as shown in Figure 5.2 to Figure 5.8.

Although the molecular size of toluene was greater than that of acetone, the former was able to be adsorbed more fast than the latter since the molecular structure of acetone consisted of large branches in comparison with the size, whereas the molecular structure of toluene was almost round as a ring as illustrated in Figure 5.19

In addition, the mass transfer coefficients increased with an increase in temperature of the system, as shown in Figure 5.20 and Figure 5.21 because of an increase in internal energy. However, the relationships between the overall mass transfer coefficients and the temperature did not quite correspond with the Arrhenius's

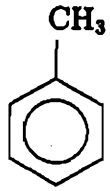

Toluene

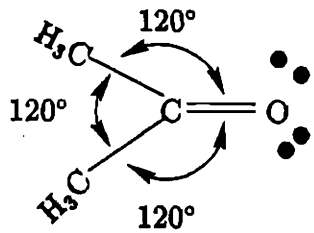

Acetone

Figure 5.19: The structure of Toluene and Acetone

Table 5.7: Axial dispersion of toluene on Perlite and Pumice Volcanic Rocks

Adsorbates	Temp °C	Pumice (mesh)			Perlite (mesh)			D_m
		40-60	60-80	80-100	40-60	60-80	80-100	
Toluene	40	0.200	0.190	0.280	0.710	1.150	0.410	0.420
	50	0.180	0.260	0.380	1.640	1.270	0.150	0.441
	60	0.370	0.300	0.380	2.220	2.450	0.120	0.466
	70	0.280	0.390	0.300	0.550	1.590	0.220	0.492
	80	0.280	0.520	0.100	0.690	1.140	0.170	0.519
	90	0.300	0.480	0.050	0.270	1.190	0.580	0.546
	100	0.410	0.660	0.050	0.240	0.440	0.160	0.574
	110	0.210	0.740	0.800	0.390	0.270	0.240	0.602
Acetone	40	0.31	0.45	0.42	2.15	6.33	9.47	0.479
	50	0.39	0.16	0.23	3.56	5.64	5.28	0.508
	60	0.36	0.21	0.31	3.05	3.83	4.55	0.537
	70	0.41	0.13	0.35	6.55	3.36	4.02	0.567
	80	0.49	0.19	0.24	6.54	5.40	1.00	0.597
	90	0.67	0.26	0.33	9.22	3.70	0.68	0.628
	100	0.30	0.35	0.28	10.00	3.95	0.48	0.660
	110	0.29	0.15	0.36	3.85	7.23	0.43	0.693

equation, except adsorption of perlite, as shown in Figure 5.22.

5.4.2 Axial Dispersion

With the second absolute moment of the chromatograms, the slope of the linear plot, according to equation 3.15, provided the information of the axial dispersion within the packed bed of adsorbents. The results were summarized in Table 5.7.

In comparison with the molecular diffusivity in helium, most obtained axial

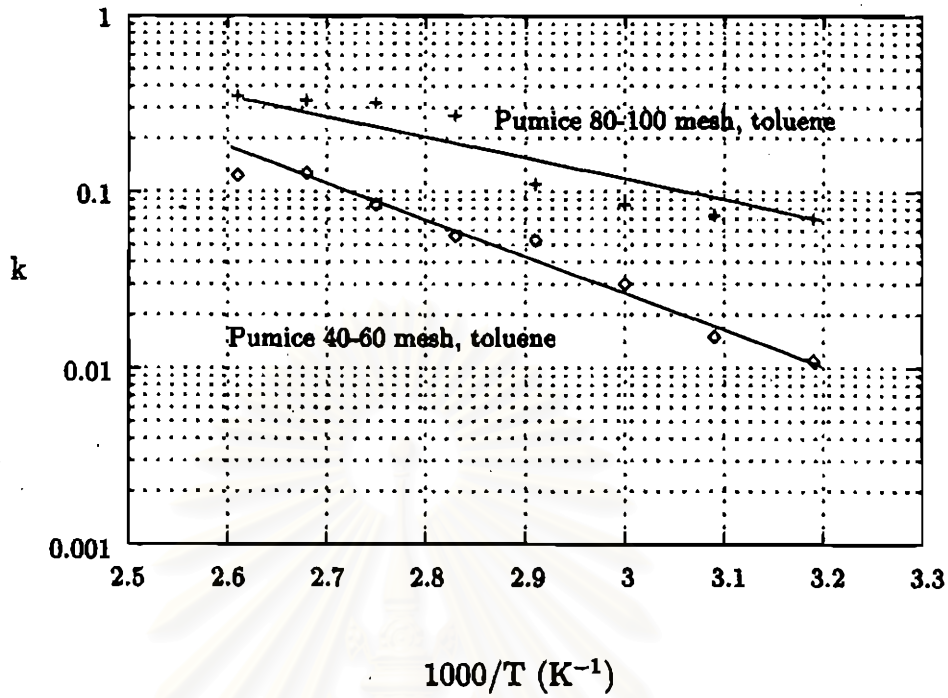

Figure 5.20: Overall mass transfer coefficients of toluene on Pumice 40-60 mesh and Pumice 80-100 mesh

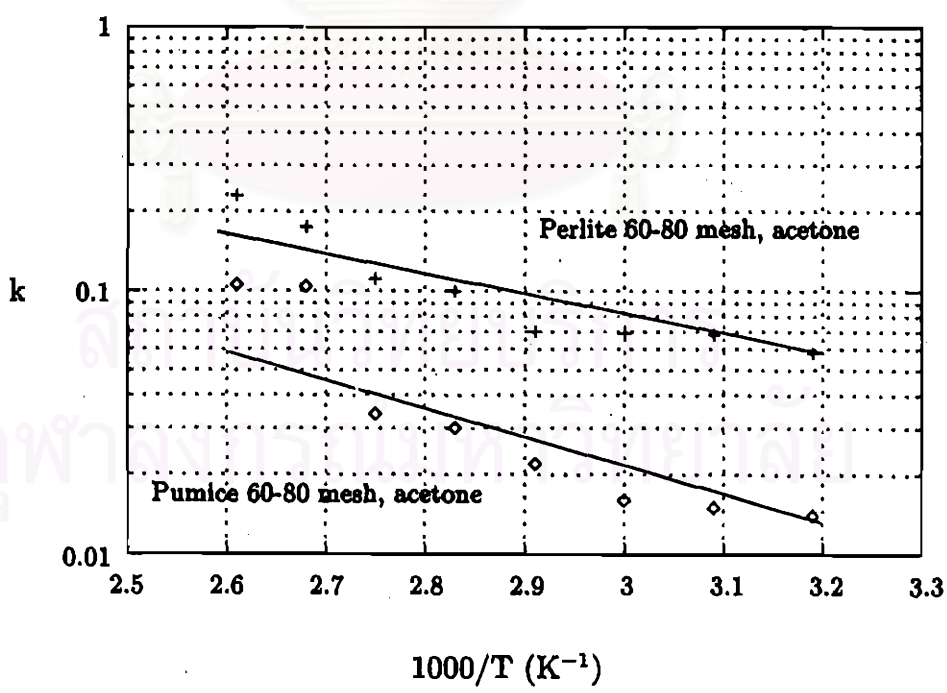

Figure 5.21: Overall mass transfer coefficients of acetone on Pumice 60-80 mesh and Perlite 60-80 mesh

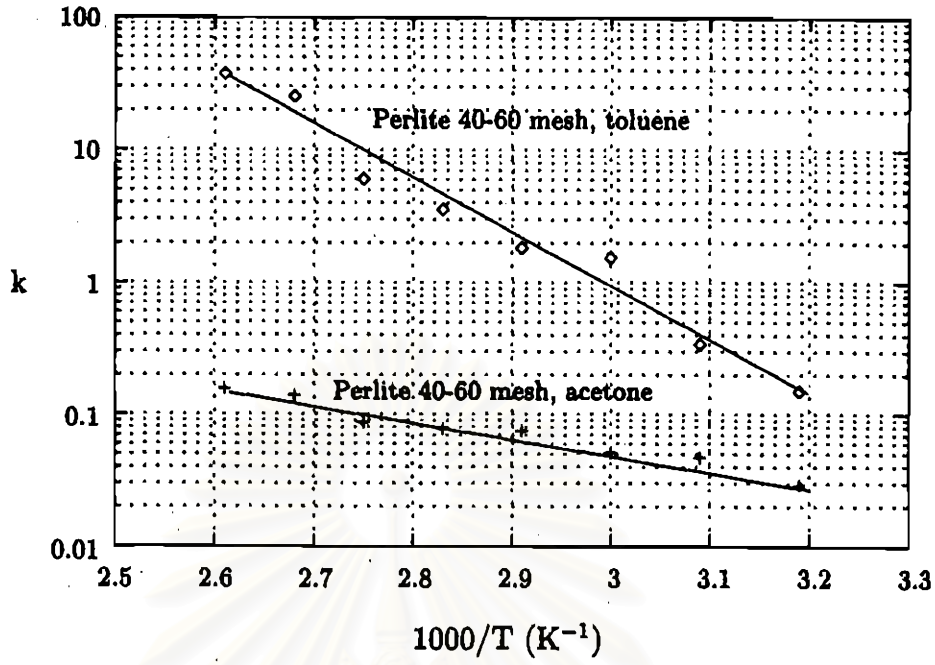

Figure 5.22: Overall mass transfer coefficients of toluene and acetone on Perlite 40-60 mesh

dispersion coefficients were less than the corresponding molecular diffusivities. The results suggested that the axial dispersion affected the propagation of the adsorbate along the bed of adsorbents slightly.